

Stochastic Dynamics of Growing Young Diagrams and Their Limit Shapes

P. L. Krapivsky¹

¹*Department of Physics, Boston University, Boston, MA 02215, USA*

We investigate a class of growing two-dimensional Young diagrams parametrized by a non-negative integer r , the minimal difference between the heights of adjacent columns. The limit shapes emerging in the long time limit are analytically determined, and fluctuations of the height and the width are briefly discussed. We also analyze the generalization to ‘diffusively’ growing Young diagrams.

I. INTRODUCTION

Partitions of integers appear in various branches of mathematics, especially in combinatorics, number theory and group representations [1–8], and also in physics [9–16]. By definition, a partition of a natural number n is its representation as a sum

$$n = m_1 + \dots + m_k, \quad m_1 \geq \dots \geq m_k > 0 \quad (1)$$

The total number of partitions of n is denoted by $p(n)$. For instance, $4 = 4$, $4 = 3 + 1$, $4 = 2 + 2$, $4 = 2 + 1 + 1$ and $4 = 1 + 1 + 1 + 1$ are all possible partitions of 4. Therefore $p(4) = 5$.

The study of partitions goes back to Euler [1]. One his famous result is the beautiful expression of the generating function encoding the sequence $p(n)$ through a neat infinite product

$$\sum_{n \geq 0} p(n) q^n = \prod_{k \geq 1} \frac{1}{1 - q^k} \quad (2)$$

(It is convenient to set $p(0) = 1$.) Using (2) one can deduce the large n asymptotic $\ln p(n) \simeq 2\pi\sqrt{n/6}$. A more precise asymptotic formula by Hardy and Ramanujan [2]

$$p(n) \simeq \frac{1}{4\sqrt{3}n} \exp\left[\pi\sqrt{\frac{2n}{3}}\right]$$

and an exact Hardy-Ramanujan-Rademacher formula [3] have been derived (see e.g. [4]) via a connection of the generating function (2) with Dedekind’s eta function.

One can think about partitions geometrically representing them by Young diagrams (Fig. 1); e.g. the Young diagram of the partition (1) has k columns, with m_j being the height of the j^{th} column. The total number $\mathbb{Y}_2(n)$ of Young diagrams composed of n elemental squares is $\mathbb{Y}_2(n) = p(n)$. Rather than fixing area, one can impose other restrictions, e.g. one can consider Young diagrams that fit into an $a \times b$ box. The total number of such diagrams is $\mathbb{Y}(a, b) = (a + b)!/[a!b!]$.

The Young diagram is a two-dimensional (lattice) object, and it admits an obvious generalization to higher dimensions. The analog of Eq. (2) is known in three (but not higher) dimensions [5, 7, 17]:

$$\sum_{n \geq 0} \mathbb{Y}_3(n) q^n = \prod_{k \geq 1} \frac{1}{(1 - q^k)^k} \quad (3)$$

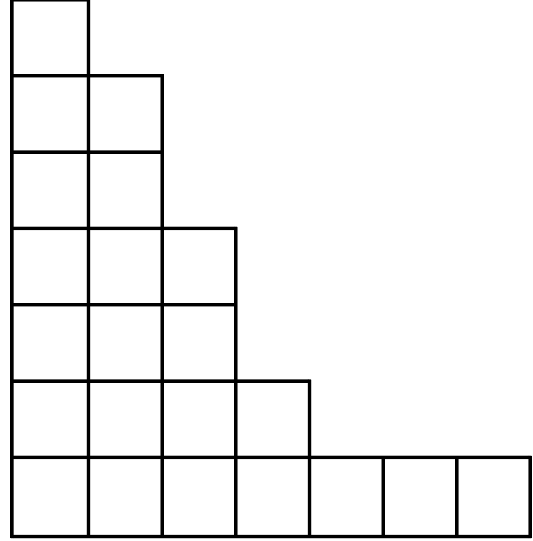


FIG. 1: A Young diagram of a partition of a positive integer n is a diagram with n boxes arranged in columns with non-increasing height. Shown is the Young diagram of the partition $22 = 7 + 6 + 4 + 2 + 1 + 1 + 1$.

where $\mathbb{Y}_3(n)$ is the total number of three-dimensional Young diagrams of ‘volume’ n . This expression via an infinite product was discovered by MacMahon [17] who also found a beautiful formula for the total number $\mathbb{Y}(a, b, c)$ of Young diagrams that fit into an $a \times b \times c$ box [7, 17]

$$\mathbb{Y}(a, b, c) = \prod_{i=1}^a \prod_{j=1}^b \prod_{k=1}^c \frac{i + j + k - 1}{i + j + k - 2} \quad (4)$$

The total number $p(n)$ of partitions rapidly grows with n , yet for large n partitions are mostly similar, namely their Young diagrams look alike. To make this assertion precise one must define the probability measure. The simplest choice is the *uniform* probability measure postulating that all $p(n)$ partitions of n are equiprobable. The limit shape emerges after rescaling the coordinates

$$X = \frac{j}{\sqrt{n}}, \quad Y = \frac{m_j}{\sqrt{n}} \quad (5)$$

and taking the $n \rightarrow \infty$ limit while keeping X and Y

There is still no difference with the equilibrium (uniform) measure.

Both partitions which are possible outcomes of the process (9) evolve with overall rate 2 and lead to

$$\bullet\bullet\bullet\bullet\bullet\bullet\circ\circ\circ\circ \implies \begin{cases} \bullet\bullet\circ\bullet\bullet\circ\circ\circ \\ \bullet\bullet\circ\bullet\bullet\circ\circ\circ \end{cases} \quad (10)$$

and

$$\bullet\bullet\bullet\bullet\circ\circ\bullet\circ\circ\circ \implies \begin{cases} \bullet\bullet\circ\bullet\bullet\circ\circ\circ \\ \bullet\bullet\bullet\circ\circ\circ\bullet\circ\circ \end{cases} \quad (11)$$

Note that the partition $3 = 2 + 1$ which has the lattice gas representation $\bullet\bullet\bullet\circ\bullet\bullet\circ\circ\circ$ occurs with probability $1/2$ while other partitions, $3 = 1 + 1 + 1$ and $3 = 3$, occur with probability $1/4$ each. Thus different partitions may come with different weights hinting, correctly, that the limit shape of growing partitions is different from the equilibrium limit shape (6).

Thus in the underlying lattice gas particles satisfy an exclusion property (at most one particle per site) and they hop to neighboring empty sites on the right with equal (unit) rates. This lattice gas is known [34, 41] as a totally asymmetric simple exclusion process (TASEP).

We now remind the derivation of the limit of growing partitions as we shall employ the same approach for other classes of growing partitions. The idea is to use the above lattice gas representation and to rely on a hydrodynamic description. This description ignores fluctuations, but it suffices for the derivation of the limit shape. The hydrodynamic description is based on a continuity equation

$$\frac{\partial n}{\partial t} + \frac{\partial J}{\partial z} = 0 \quad (12)$$

for the average density $n(z, t)$. For the TASEP, the current $J(n)$ has a very simple form [34, 41]

$$J(n) = n(1 - n) \quad (13)$$

Equations (12)–(13) subject to the initial condition (7), equivalently

$$n(z, 0) = \begin{cases} 1 & z < 0 \\ 0 & z > 0 \end{cases} \quad (14)$$

admit a scaling solution, $n(z, t) = N(Z)$ with $Z = z/t$. The scaled density profile is

$$N(Z) = \begin{cases} 1 & Z < -1 \\ \frac{1}{2}(1 - Z) & |Z| < 1 \\ 0 & Z > 1 \end{cases} \quad (15)$$

This is a simple example of a rarefaction wave. Rarefaction waves are among the simplest solutions of hyperbolic partial differential equations, they help to understand the basic features of driven lattice gases (see e.g. [39, 41]).

The limit shape is determined from the density through relation

$$y(x, t) = \int_{x-y}^{\infty} dz n(z, t) \quad (16)$$

Rescaling the coordinates

$$X = \frac{x}{t}, \quad Y = \frac{y}{t} \quad (17)$$

we re-write (16) as

$$Y = \int_{\max(X-Y, -1)}^1 dZ N(Z) \quad (18)$$

Combining (15) and (18) we obtain an implicit equation for the limit shape

$$4Y = \begin{cases} 1 - 2(X - Y) + (X - Y)^2 & |X - Y| < 1 \\ 0 & X - Y > 1 \end{cases}$$

This equation can be recast into a manifestly symmetric form [33]

$$\sqrt{X} + \sqrt{Y} = 1 \quad (19)$$

in the region $0 < X, Y < 1$.

III. GROWING YOUNG DIAGRAMS WITH UNEQUAL PARTS

Partitions with the requirement that all parts are unequal, known as strict partitions, were already studied by Euler [1] who expressed the generating function for such partitions through an infinite product

$$\sum_{n \geq 0} p_1(n) q^n = \prod_{k \geq 1} (1 + q^k) \quad (20)$$

Here the convention $p_1(0) = 1$ is used again; the index in the partition function $p_1(n)$ reminds about the requirement $m_j - m_{j+1} \geq 1$. For instance $6 = 6$, $6 = 5 + 1$, $6 = 4 + 2$, $6 = 3 + 2 + 1$ are the only partitions of 6 with unequal parts, so $p_1(6) = 4$; the number of arbitrary partitions of 6 is $p(6) = 11$. Using (20) and analyzing the $q \rightarrow 1$ behavior one can extract the asymptotic behavior: $\ln p_1(n) \simeq \pi\sqrt{n/3}$ as $n \rightarrow \infty$. A more comprehensive analysis [5] gives the Ramanujan asymptotic formula

$$p_1(n) \simeq \frac{1}{4 \cdot 3^{1/4} n^{3/4}} \exp\left[\pi\sqrt{\frac{n}{3}}\right]$$

The limit shape of partitions with unequal parts chosen uniformly among all $p_1(n)$ partitions has been established in Ref. [21] using the generating function (20). In the rescaled coordinates (5) this limit shape reads

$$e^{\lambda X} - e^{-\lambda Y} = 1, \quad \lambda = \frac{\pi}{\sqrt{12}} \quad (21)$$

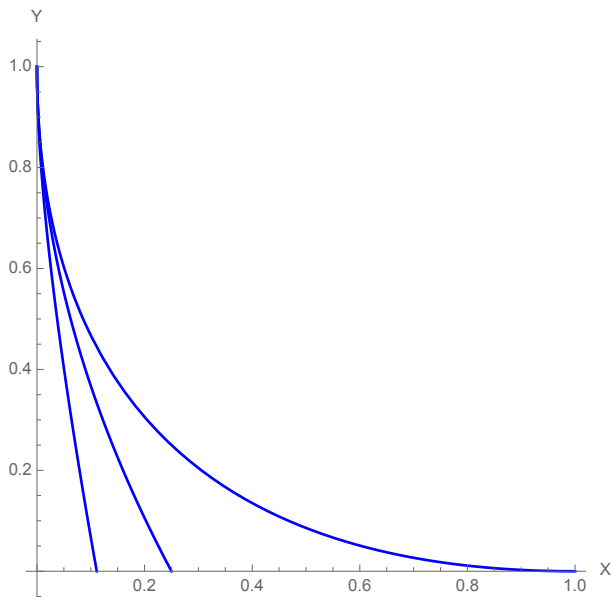


FIG. 3: Plotted (top to bottom) are the limit shapes with $r = 0, 1, 4$. They are given by Eq. (35); the first two limit shapes also appear as (19) and (27).

Let us analyze growing r -strict partitions. The first unexplored case is $r = 2$. In this model the first deposition event is described by (8), the second by (23), the third deposition event is still unique

$$\bullet \bullet \bullet \bullet \bullet \circ \circ \circ \circ \circ \circ \Rightarrow \bullet \bullet \bullet \bullet \bullet \circ \circ \circ \circ \quad (30)$$

and only then there are two possible outcomes

$$\bullet \bullet \bullet \bullet \bullet \circ \circ \circ \circ \circ \circ \Rightarrow \begin{cases} \bullet \bullet \bullet \bullet \bullet \circ \circ \circ \circ \\ \bullet \bullet \bullet \bullet \bullet \circ \circ \circ \circ \end{cases} \quad (31)$$

Analyzing (8), (23), (30) and (31) we see that the underlying lattice gas is a facilitated asymmetric simple exclusion process FTASEP(2) where a particle can hop only when it is pushed from the left by two adjacent particles.

Generally r -strict growing partitions are mapped onto the FTASEP(r), an exclusion process in which the push by r adjacent particles from the left is required for the hop to the neighboring empty site on the right. Remarkably, the current is known (see [42–48] and references therein) for all such processes:

$$J(n) = \frac{(1-n)[(r+1)n-r]}{rn+1-r} \quad (32)$$

The following analysis is a straightforward (although a bit lengthy) extension of the approach described before, so we merely present final results. The non-trivial part of the density

$$N(Z) = 1 - r^{-1} + r^{-1}[1 + r + rZ]^{-1/2} \quad (33)$$

is valid in the region

$$-1 < Z < V(r), \quad V(r) = \frac{1}{(\sqrt{r}+1)^2} \quad (34)$$

For $Z < -1$ and for $Z > V(r)$ the density profile remains unperturbed. The non-trivial part of the limit shape is surprisingly simple:

$$Y = 1 - 2\sqrt{X} - (r-1)X, \quad 0 < X < V(r) \quad (35)$$

In the original coordinates

$$y_{\max} = t, \quad x_{\max} = V(r)t = \frac{t}{(\sqrt{r}+1)^2} \quad (36)$$

We also note that the area under the parabola (35) is

$$A(r) = \frac{3\sqrt{r}+1}{6(\sqrt{r}+1)^3} \quad (37)$$

In the original coordinates, the area is $A(r)t^2$. Note that the area is a decreasing function of r .

V. FLUCTUATIONS OF THE HEIGHT AND THE WIDTH OF GROWING YOUNG DIAGRAMS

Having established a limit shape, one would also like to determine fluctuations around it. Our understanding of fluctuations of growing interfaces has greatly improved in last 30 years (see [52–55] for review), particularly for one-dimensional interfaces [53, 54]. The corner growth process played a crucial role as the first example where fluctuations were understood [56]. Using the mapping of the corner growth process onto the TASEP one can explore fluctuations in the latter framework. Let us start with the initial condition (7) and count the integrated current, i.e. the number of particles P_t which enter the initially empty half-line $x \geq 0$ at time t . Since the density is asymptotically $n = \frac{1}{2}$ at the origin, see (15), the current is $n(1-n) = 1/4$ and the average integrated current is $t/4$. The more precise behavior is [56]

$$P_t = \frac{t}{4} + t^{1/3}\mathcal{F}_{GUE} \quad (38)$$

where \mathcal{F}_{GUE} is the Tracy-Widom GUE distribution (the GUE abbreviation reflects that it arises in the Gaussian unitary ensemble of random matrices). Noting that the interface in the corner growth process intersects the diagonal at the point (P_t, P_t) we see that fluctuations of the random quantity P_t are directly related to fluctuations of the interface in the (1, 1) direction. The same fluctuations occur in other directions, only the amplitude depends on the direction [53, 54]. The only exceptions are the horizontal and vertical directions. Fluctuations of the width and height in the corner growth process are Gaussian. This becomes evident in the lattice gas representation. For instance, the width is the displacement of the right-most particle which is independent on other particles, it merely hops to the right with unit rate. Therefore the width w_t has the Poisson distribution

$$\text{Prob}(w_t = n) = \frac{t^n}{n!} e^{-t} \quad (39)$$

which is asymptotically Gaussian with fluctuation on the scale $t^{1/2}$. Similarly the height is the displacement of the left-most vacancy, so it has the same Poisson distribution.

We now return to growing strict partitions and discuss fluctuations of the height and of the width. The former behaves as in the corner growth process:

$$\text{Prob}(h_t = n) = \frac{t^n}{n!} e^{-t} \quad (40)$$

The behavior of the width is harder to quantify since the right-most particle in the FTASEP hops only when it is pushed by its neighbor. Let us map the FTASEP onto a lattice gas [57, 58] in which a site corresponds to adjacent particles in the FTASEP, and it is empty (\square) if adjacent particles are nearest neighbors and occupied (\blacksquare) if there is a vacancy between adjacent particles. This is a one-to-one mapping since starting with initial condition (7) adjacent particles in the FTASEP will be separated by at most one vacancy. Note also that (7) corresponds to the empty half-line in the new lattice gas, see (41). Here is an example of the evolution (time goes from top to bottom)

$$\begin{array}{ll} \dots \bullet \bullet \bullet \bullet \bullet \bullet \circ \circ \circ \dots & \dots \square \square \square \square \\ \dots \bullet \bullet \bullet \bullet \bullet \circ \circ \circ \dots & \dots \square \square \square \blacksquare \\ \dots \bullet \bullet \bullet \bullet \circ \bullet \circ \circ \dots & \dots \square \square \square \blacksquare \\ \dots \bullet \bullet \bullet \circ \bullet \circ \bullet \circ \dots & \dots \square \square \blacksquare \blacksquare \\ \dots \bullet \bullet \bullet \circ \bullet \circ \bullet \circ \dots & \dots \square \blacksquare \square \blacksquare \\ \dots \bullet \bullet \circ \bullet \bullet \circ \bullet \circ \dots & \dots \square \blacksquare \square \blacksquare \\ \dots \bullet \bullet \circ \bullet \bullet \circ \bullet \circ \dots & \dots \square \blacksquare \square \blacksquare \end{array} \quad (41)$$

The lattice model shown on the right is the half-TASEP with particles hopping to the left and new particles entering the right-most site (both processes occur with unit rate). A simple but crucial observation immediately following from the above example is that the displacement w_t of the right-most particle for the FTASEP is the same as the total number of particles (denoted by \blacksquare) in the half-TASEP.

For the TASEP starting with the initial condition (7) the total number of particles entering initially empty half line is given by (38). For the half-TASEP one expects that the total number of particles w_t entering initially empty half-line behaves similarly to (38). Fluctuations scale indeed as $t^{1/3}$, but they follow [58] the GSE Tracy-Widom distribution related to the Gaussian symplectic ensemble of random matrices:

$$w_t = \frac{t}{4} + t^{1/3} \mathcal{F}_{GSE} \quad (42)$$

The same \mathcal{F}_{GSE} appears in other growth processes in half-line [59–61], while the \mathcal{F}_{GUE} distribution describes fluctuations of the leading particle in a process studied in Ref. [62].

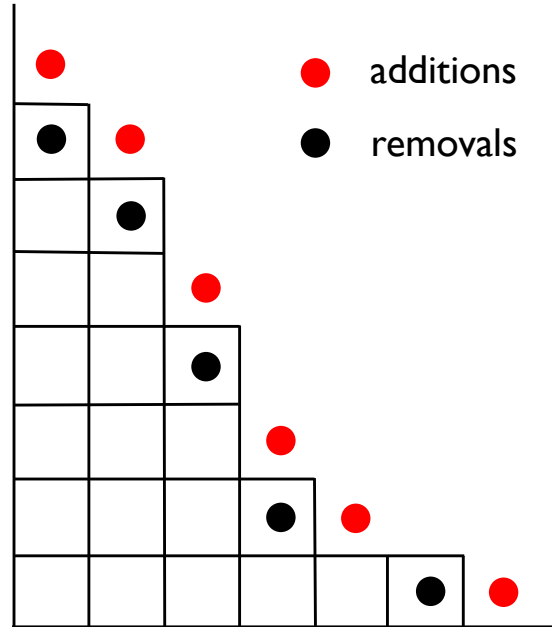


FIG. 4: Diffusive growth of arbitrary partitions—additions and removals of squares occur with the same rate. Shown is the Young diagram of the partition $21 = 7 + 6 + 4 + 2 + 1 + 1$ together with 6 spots to which a square can be added and 5 spots from which squares can be removed. There is always one more spot for addition than for removal, so the average the area is $\langle S \rangle = t$ implying that the typical size grows diffusively as \sqrt{t} .

VI. DIFFUSIVE GROWTH

In the previous sections we considered growing partitions (only deposition events were allowed). We investigated partitions of different types: arbitrary partitions, partitions with unequal parts (strict partitions), and generally partitions with height difference $\geq r$. The growth was always ballistic, see (36).

One can allow both additions and removals of squares, requiring of course that the evolving Young diagram remains the Young diagram of the prescribed type. If the addition rate exceeds the evaporation rate, the growth remains ballistic. A qualitatively different diffusive growth occurs if additions and removals of squares proceed with equal rates. Figure 4 illustrates this process in the case of arbitrary partitions. The number of positions where new squares can be added always exceeds by one the number of positions from which squares can be removed. Hence the average area increases linearly in time:

$$\langle S \rangle = t \quad (43)$$

In the case of arbitrary partitions the above evolution process maps onto the symmetric simple exclusion process (SSEP) for which the diffusion equation, $n_t = n_{zz}$,

The boundary conditions on the right edge are

$$N(v) = \frac{r}{r+1}, \quad N'(v) = -v \frac{2r}{(r+1)^3} \quad (55)$$

Numerically solving (54) subject to (48) and (55) one can find $v = v(r)$.

Finally, let us discuss fluctuations. In the case of arbitrary partitions the mapping onto the SSEP is a significant simplification since fluctuations in lattice gases with constant diffusion coefficients are more amenable to analytical treatment (see [63, 64] for a review of fluctuations in diffusive lattice gases). Fluctuations in the FSSEP, and generally in lattice gases with density-dependent diffusion coefficients, are very challenging.

For arbitrary diffusively growing partitions one can probe fluctuations of the area [38]. These fluctuations turn out to be strongly non-Gaussian. The cumulants grow as $\langle S^p \rangle_c = A_p t^{(p+1)/2}$ in the $t \rightarrow \infty$ limit. For $p \leq 4$, the amplitudes A_p have been determined analytically [38]. For diffusively growing strict partitions one can try to generalize the perturbative approach [65] to the determination of the variance and extend the computations of Ref. [38] to strict partitions. This is perhaps doable, although the lack of explicit analytical solution to (47) possesses an extra challenge.

Fluctuations of the width and height might be more tractable. In the case of arbitrary partitions, the average displacement of the right-most particle can be estimated from the criterion

$$\int_{\langle w_t \rangle}^{\infty} dz n(z, t) \sim 1 \quad (56)$$

Combining (44) and (56) one gets

$$\langle w_t \rangle \simeq \sqrt{2t \ln t} \quad (57)$$

One can heuristically estimate the variance of the width, $\langle w_t^2 \rangle - \langle w_t \rangle^2$, by arguing that it scales as the square of the average gap $\langle g_t \rangle$ between the right-most particle and the following particle. This gap can be estimated from the criterion $\int_{\langle w_t \rangle - \langle g_t \rangle}^{\langle w_t \rangle} dz n(z, t) \sim 1$ to give

$$\langle w_t^2 \rangle - \langle w_t \rangle^2 \sim \frac{t}{\ln t} \quad (58)$$

More precise results are available in the situation when particles undergo Brownian motions [66], while the relevant case of the SSEP is studied in [67].

In the case of strict diffusively growing Young diagrams we use again the mapping illustrated in (41), now it is the mapping of the FSSEP onto the half-SSEP. A similar model has been studied in the past—the SSEP with a localized source, more precisely the infinitely strong source into the origin [68–71]. The average number of particles in the half-SSEP, which is identical to the average width of strict diffusively growing Young diagrams, is easy to compute: $\langle w_t \rangle \simeq 2\sqrt{t/\pi}$. The variance (computed in [68, 69] using more advanced techniques) is

$$\langle w_t^2 \rangle - \langle w_t \rangle^2 \simeq 2(3 - \sqrt{8})\sqrt{t/\pi} \quad (59)$$

Therefore fluctuations scale as $t^{1/4}$ and

$$w_t = 2\sqrt{t/\pi} + t^{1/4}\mathcal{W} \quad (60)$$

The challenge is to determine the (non-Gaussian) random distribution \mathcal{W} .

VII. CONCLUDING REMARKS

We computed limit shapes for an infinite family of growing two-dimensional Young diagrams parametrized by a non-negative integer r , the minimal difference between the heights of adjacent columns. In the situation when additions and removals of squares proceed with equal rates, the growth is diffusive; we determined the corresponding limit shapes, although not explicitly as they are expressed through analytically insoluble ordinary differential equations.

Generally, limit shapes characterizing growing objects are often computable. For instance, infinitely many limit shapes were computed [37] for the melting Ising crystals on the square lattice with ferromagnetic spin-spin interactions; these limit shapes are parametrized by the range of interaction. The major challenge is the extension to the three-dimensional growing Young diagrams. The mapping of the growing interface in three dimensions onto a two-dimensional lattice gas is possible, but it has not yet led to a scheme allowing to extract a limit shape.

I am grateful to K. Mallick for useful discussions. I also benefitted from the correspondence with G. Barraquand, I. Corwin, K. Mallick and T. Sasamoto. This work was supported by the BSF Grant No. 2012145.

-
- [1] L. Euler, *Introduction to Analysis of the Infinite* (Springer, New York, 1988).
 [2] G. H. Hardy and S. Ramanujan, Proc. London Math. Soc. **17**, 75 (1918).
 [3] H. Rademacher, Proc. London Math. Soc. **43**, 241 (1937).
 [4] T. M. Apostol, *Modular Functions and Dirichlet Series*

- in Number Theory*, 2nd ed. (Springer-Verlag, New York, 1990).
 [5] G. E. Andrews, *The Theory of Partitions* (Cambridge University Press, New York, 1976).
 [6] W. Fulton, *Young Tableaux, with Applications to Representation Theory and Geometry* (Cambridge University

- Press, New York, 1997).
- [7] I. G. Macdonald, *Symmetric Functions and Hall Polynomials* (Oxford University Press, Oxford, 1999).
- [8] D. Romik, *The Surprising Mathematics of Longest Increasing Subsequences* (Cambridge University Press, New York, 2015).
- [9] H. A. Bethe, *Phys. Rev.* **50**, 332 (1936).
- [10] H. N. V. Temperley, *Proc. R. Soc. A* **199**, 361 (1949).
- [11] F. Y. Wu, G. Rollet, H. Y. Huang, J. M. Maillard, C. K. Hu, and C. N. Chen, *Phys. Rev. Lett.* **76**, 173 (1996).
- [12] M. N. Tran, M. V. N. Murthy, and R. K. Bhaduri, *Ann. Phys.* **311**, 204 (2004).
- [13] A. Kubasiak, J. K. Korbicz, J. Zakrzewski, and M. Lewenstein, *EPL* **72**, 506 (2005).
- [14] A. Comtet, S. N. Majumdar, and S. Ouvry, *J. Phys. A* **40**, 11255 (2007).
- [15] N. Destainville and S. Govindarajan, *J. Stat. Phys.* **158**, 950 (2015).
- [16] A. Okounkov, *Bull. Amer. Math. Soc.* **53**, 187 (2016).
- [17] P. A. MacMahon, *Combinatory analysis*, Vol. I & II (Cambridge University Press, Cambridge, 1915–16).
- [18] H. N. V. Temperley, *Proc. Cambridge Philos. Soc.* **48**, 683 (1952).
- [19] A. M. Vershik and S. V. Kerov, *Funct. Anal. Appl.* **19**, 21 (1985).
- [20] J.-P. Marchand and Ph. A. Martin, *J. Stat. Phys.* **44**, 491 (1986).
- [21] A. M. Vershik, *Funct. Anal. Appl.* **30**, 90 (1996); A. M. Vershik, *J. Math. Sci.* **119**, 165 (2004).
- [22] A. M. Vershik and Yu. V. Yakubovich, *Moscow Math. J.* **1**, 457 (2001).
- [23] S. Shlosman, *J. Math. Phys.* **41**, 1364 (2000).
- [24] P. L. Krapivsky, S. Redner, and J. Tailleur, *Phys. Rev. E* **69**, 026125 (2004).
- [25] A. M. Vershik and S. V. Kerov, *Soviet Math. Dokl.* **18**, 527 (1977).
- [26] R. Cerf and R. Kenyon, *Commun. Math. Phys.* **222**, 147 (2001).
- [27] A. Okounkov and N. Reshetikhin, *J. Amer. Math. Soc.* **16**, 581 (2003).
- [28] H. Cohn, M. Larsen, and J. Propp, *New York J. Math.* **4**, 137 (1998).
- [29] H. Cohn, R. Kenyon, and J. Propp, *J. Amer. Math. Soc.* **14**, 297 (2001).
- [30] A. Okounkov and N. Reshetikhin, *Commun. Math. Phys.* **269**, 571 (2007).
- [31] R. Kenyon and A. Okounkov, *Acta Math.* **199**, 263 (2007).
- [32] P. Di Francesco and N. Reshetikhin, *Commun. Math. Phys.* **309**, 87 (2012).
- [33] H. Rost, *Theor. Prob. Rel. Fields* **58**, 41 (1981).
- [34] T. M. Liggett, *Interacting Particle Systems* (Springer, New York, 1985).
- [35] D. Kandel and E. Domany, *J. Stat. Phys.* **58**, 685 (1990).
- [36] M. Barma, *J. Phys. A* **25**, L693 (1992).
- [37] P. L. Krapivsky and J. Olejarz, *Phys. Rev. E* **87**, 062111 (2013).
- [38] P. L. Krapivsky, K. Mallick, and T. Sadhu, *J. Phys. A* **48**, 015005 (2015).
- [39] P. L. Krapivsky, S. Redner and E. Ben-Naim, *A Kinetic View of Statistical Physics* (Cambridge: Cambridge University Press, 2010).
- [40] P. L. Krapivsky, *Phys. Rev. E* **85**, 011152 (2012).
- [41] R. A. Blythe and M. R. Evans, *J. Phys. A* **40**, R333 (2007).
- [42] T. Sasamoto and M. Wadati, *J. Phys. A* **31**, 6057 (1998).
- [43] K. Klauk and A. Schadschneider, *Physica A* **271**, 102 (1999).
- [44] T. Antal and G. M. Schütz, *Phys. Rev. E* **62**, 84 (2000).
- [45] G. Lakatos and T. Chou, *J. Phys. A* **36**, 2027 (2003).
- [46] L. B. Shaw, R. K. P. Zia, and K. H. Lee, *Phys. Rev. E* **68**, 021910 (2003).
- [47] U. Basu and P. K. Mohanty, *Phys. Rev. E* **79**, 041143 (2009).
- [48] A. Gabel, P. L. Krapivsky, and S. Redner, *Phys. Rev. Lett.* **105**, 210603 (2010).
- [49] A. Comtet, S. N. Majumdar, S. Ouvry, and S. Sabhapandit, *J. Stat. Mech.* (2007) P10001.
- [50] A. Comtet, S. N. Majumdar, and S. Sabhapandit, *J. Math. Phys. Anal. Geom.* **4**, 24 (2008).
- [51] P. L. Krapivsky, *J. Stat. Mech.* P06012 (2013).
- [52] T. Halpin-Healy and Y.-C. Zhang, *Phys. Rep.* **254**, 215 (1995).
- [53] M. Prähofer and H. Spohn, “Current fluctuations for the totally asymmetric exclusion process,” pp. 185–204 in: *In and Out of Equilibrium: Probability with a Physics Flavor*, ed. by V. Sidoravicius (Birkäuser, Boston, 2006).
- [54] I. Corwin, *Random Matrices Theory Appl.* **1**, 1130001 (2012).
- [55] T. Halpin-Healy and K. A. Takeuchi, *J. Stat. Phys.* **160**, 794 (2015).
- [56] K. Johansson, *Commun. Math. Phys.* **209**, 437 (2000).
- [57] K. Mallick, unpublished.
- [58] J. Baik, G. Barraquand, I. Corwin, and T. Suidan, “Facilitated exclusion process and pfaffian Schur processes,” preprint.
- [59] J. Baik and E. M. Rains, *Duke Math. J.* **109**, 1 (2001) and *Duke Math. J.* **109**, 205 (2001).
- [60] J. Baik and E. M. Rains, “Symmetrized random permutations,” pp. 1–19 in: *Random matrix models and their applications* (Cambridge: Cambridge University Press, 2001).
- [61] T. Sasamoto and T. Imamura, *J. Stat. Phys.* **115**, 749 (2004); T. Sasamoto, *J. Stat. Mech.* P07007 (2007).
- [62] G. Barraquand and I. Corwin, arXiv:1501.03445.
- [63] B. Derrida, *J. Stat. Mech.* P07023 (2007).
- [64] L. Bertini, A. De Sole, D. Gabrielli, G. Jona-Lasinio, and C. Landim, *Rev. Mod. Phys.* **87**, 593 (2015).
- [65] P. L. Krapivsky and B. Meerson, *Phys. Rev. E* **86**, 031106 (2012).
- [66] S. Sabhapandit, *J. Stat. Mech.* L05002 (2007).
- [67] K. Mallick and T. Sasamoto, in preparation.
- [68] J. E. Santos and G. M. Schütz, *Phys. Rev. E* **64**, 036107 (2001).
- [69] P. L. Krapivsky, *Phys. Rev. E* **86**, 041103 (2012).
- [70] C. A. Tracy and H. Widom, *J. Math. Phys.* **54**, 103301 (2013).
- [71] P. L. Krapivsky and D. Stefanovic, *J. Stat. Mech.* P09003 (2014).